Engineering

Mechanical Engineering fields

Okayama University *Year* 2002

Pneumatic direct-drive stepping motor for robots

Koichi Suzumori* Tatsuya Hashimoto†

Kazuo Uzuka‡ Isao Enomoto**

*Okayama University

†Okayama University

‡TOK Bearings Corporation Limited

**TOK Bearings Coｒporation Limited

Proceedings of the 2002 IEEE/RSJ
Intl. Conference on Intelligent Robots and Systems
EPFL, Lausanne, Switzerland • October 2002

Pneumatic Direct-drive Stepping Motor for Robots

Koichi Suzumori [1], Tatsuya Hashimoto [1],
Kazuo Uzuka [2], Isao Enomoto [2]

[1] Okayama University, Okayama, Japan, suzumori@sys.okayama-u.ac.jp
[2] TOK Bearings Co. LTD., Tokyo, Japan

Abstract

A new type of pneumatic stepping motor, named pneumatic nutation motor was developed. This motor achieves stepping positioning of 720 steps/ rotation without any electrical devices or sensors mounted on the servo mechanisms. This makes the motor possible to be used under hazard conditions such as in water and in the strong magnetic fields where conventional electromagnetic motors cannot be used. The motor torque is so big that the motor can be used as a direct motor.

In this report, first, the driving principle and design of this motor are presented. Next, its characteristics are analyzed experimentally and theoretically. The motors were applied to a parallel linkage mechanism with six degrees of freedom. The mechanism shows that the pneumatic nutation motors can be used as a direct servo motor for robot mechanisms.

1. Introduction

Although conventional pneumatic actuators are unsuitable for uses of precise positioning or speed control because of air compressibility and friction of seal parts, some new pneumatic motors including reduction gear mechanism have a potential to work as a direct stepping motor for robots.

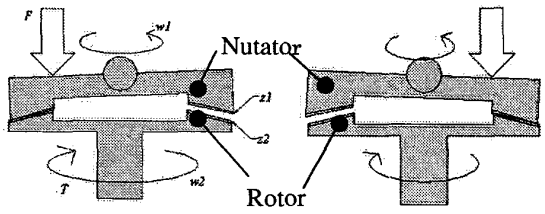

Fig.1 Driving principle of nutation motors

One of the authors has developed a pneumatic wobble motor consisting of a pair of cycloid reduction gears and a rubber wobble generator [1]. H.Kimura et al. have developed a motor consisting of a pair of crown gears and pneumatic cylinders [2]. These motors work as a pneumatic stepping motor with big torque.

In this paper, a new design of pneumatic motor and its application to parallel robot mechanism are reported. This motor consists of a pair of bevel gears and three pneumatic cylinders. It achieves gear meshing with high efficiency, resulting in small noise and vibration. In addition, the motors realize a robot servo mechanism which needs no sensors or electrical devices mounted on the robot. This shows a potential of the motor to realize robots working under hazard conditions where conventional electrical motors don't work.

2. Mechanism and Control

2.1 Mechanism

Figure 1 shows the basic driving principle of the pneumatic nutation motor. The pneumatic nutation motor consists of a pair of bevel gears; a cone-shaped bevel gear, named nutator and a cup-shaped bevel gear, named rotor. While the rotor is supported by bearings, the nutator is supported by a spherical bearing and guide pins, allowing its nutation as shown in Fig. 1. As the bevel gears have different number of tooth, nutation of the nutator causes rotation of the rotor. The motor has three pneumatic cylinders that act on the nutator as shown by the arrows in Fig. 1. Applying pressure to each cylinder sequentially causes nutation of the nutator that, in turn, causes the rotor to rotate.

Thus, a nutation motor operates by converting nutation of the nutator caused by the linear motion of the pneumatic cylinders into rotation of the rotor. This

driving principle results in the following features: 1. big torque, 2. stable motion at low-speed operation, 3. stepping control.

2. 2 Gear design

The relation between the rotational speed of the rotor, ω_r and the nutation speed of the nutator, ω_n is obtained as follows;

$$\omega_r/\omega_n=(z_r-z_w)/z_r \quad (1)$$

where z_r and z_w represent the tooth numbers of the rotor and the nutator, respectively. The value of Eq. (1) is negative. This means that the rotor rotates in the direction opposite to the direction of the nutator nutation.

2.3 Control

The two typical pressurizing patterns, i.e., full-pitch drive and half-pitch drive, are shown in Fig. 2. Solenoid valves are used for pressure control, and "1" represents pressurizing and "0" means non-pressurizing.

Full-pitch drive shifts the pressurizing pattern step by step while keeping the number of the pressurized cylinders constant. The duty ratio τ is defined as n/m, where m and n represent the number of the cylinders pressured at the same time, respectively. Then, the resolution of the nutator nutation becomes m.

Half-pitch drive changes the numbers of the pressurized chambers as shown in Fig. 2 (b), achieving the nutation resolution of $2\times m$.

CH.	1	2	3
	1	0	0
	0	1	0
time	0	0	1

(a) Full pitch drive

CH.	1	2	3
	1	0	0
	1	1	0
time	0	1	0
	0	1	1
	0	0	1
	1	0	1

(b) Half pitch drive

Fig. 2 Driving patterns

As the nutation speed of the nutator is $f\, z_r/(\, z_r - z_n)$, a step period of a pressurizing pattern, t_1 is

$$t_1= \begin{cases} (z_n - z_r)/(\, z_r f m) & \text{for full-pitch drive} \\ (z_n - z_r)/(2\, z_r f m) & \text{for half-pitch drive.} \end{cases} \quad (2)$$

where f represents the rotational speed of the motor.

3. Theoretical analysis

Figure 3 shows a model for the theoretical analysis where cylinder A is retreating and cylinder B is extending. Points O, C, and C' represent the center of the nutator, the contact point of the nutator and the rotor, and the projection of the point C onto the plane ABO, respectively. The points A and B represent the contact point of the nutator and the pistons of the cylinders A and B. r_0 and r_2 represent the distance of AO or BO, and the radius of the gear contact circle, respectively.

The nutator received force F_1 at point B from cylinder B, which is calculated as follows;

$$F_1 = p\, \pi\, r_p^2 \quad (3)$$

where r_p and p represent the radius of the cylinder bore and the applied pneumatic pressure.

Fore F_1 results in the contact fore F_H at point C as shown in Fig. 3. F_H is calculated as follows;

$$F_H = \cos\{(\psi-\theta)/2\}\, F_1\, r_0 / r_2 \quad (4)$$

where ψ represents the angle between the cylinders, the angle AOB as shown in Fig. 3 (a), and θ represents the angle which shows the contact point C', the angle AOC' as shown in Fig. 3 (a).

The relation between the torque of the rotor T and the gear meshing force in the rotational direction t, which are shown in Fig.3 (b) is obtained as follows;

$$t = T / r_2 \quad (5)$$

Figure 3 (b) shows the gear meshing of the nutator and rotor. From a kinematical analysis based on this figure, the following equations are obtained.

$$t_1 = t \cos\alpha \quad (6)$$
$$t_2 = t_1 \sin\alpha \quad = t \sin(\alpha/2) \quad (7)$$

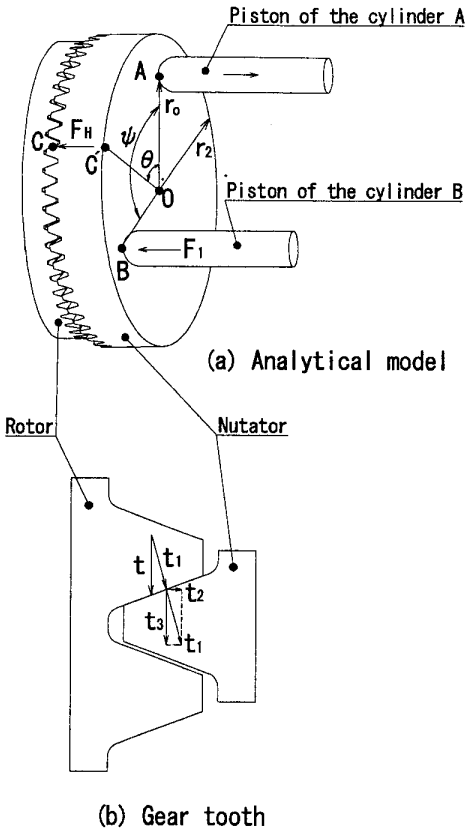

Fig. 3 Analytical model for nutation motor

$$t_3 = t_1 \cos\alpha \quad = t \cos^2\alpha \tag{8}$$

where t_1, t_2, and t_3 represent the force components in the nominal direction of the tooth, in the axial direction and in the rotational direction, respectively, as shown in the Fig. 3 (b). α represents the pressure angle of the teeth.

Friction force on the gear surfaces F_G is shown as follows;

$$F_G = \mu_1 t_1 \tag{9}$$

where μ_1 represents the coefficient of friction between the gear surfaces.

Equation (9) leads the following equations.

$$F_2 = F_G \cos\alpha \quad = \mu_1 t_1 \cos\alpha \tag{10}$$

$$F_3 = F_G \sin\alpha \quad = \mu_1 t_1 \sin\alpha \tag{11}$$

where F_2 and F_3 represent the components of the friction force in the axial direction and in the rotational direction, respectively.

Friction occurs also between the guide pins and slots. The guide pins are used to prevent the rotation of the nutator. The normal force between the guide pins and slots, N, is obtained as follows;

$$N = (t_3 + F_3)\, r_2 / r_m / K \tag{12}$$

where r_m represents the distance between the center of the nutator and the contact point of the guide pins and slots, and K represents the number of the guide pins.

Equation (12) leads the friction force between the guide pins and slots , F_M as follows;

$$F_M = \mu_2 N \tag{13}$$

where μ_2 represents the coefficient of friction between the guide pins and slots.

When the load torque exceeds a critical value, the tooth of the nutator sometimes goes over the rotor tooth, causing a slip between the rotor and the nutator. This phenomenon is observed with other type of pneumatic motors with reduction gear mechanisms. The authors call this phenomenon ratcheting [1]. Ratcheting condition corresponds to the axial force balance acting on the nutator tooth; if resultant force acting on the nutator in the axial direction is positive, ratcheting occurs, while if it is negative, ratcheting doesn't occur. This leads the following condition under which ratcheting occurs.

$$F_H < t_2 \quad + F_2 + F_M \tag{14}$$

Ratcheting is not always undesirable but is sometimes useful to protect robots and workpieces from damage. For example when a robot is accidentally subjected to a big load or impact, the motor is back-driven to release the force. Whether or not the motor is designed to have ratcheting depends on the design policy and on the nature of the applications.

4. Prototype and experiments

4.1 Designs of prototype

The prototype of the motor is shown in Figs. 4, 5, and 6. Figure 4 shows a cross-section of the motor, Fig.5 shows an external view of the motor, and Fig. 6 shows a disassembled motor.

Table 1 shows the specification of the bevel gears. The difference of tooth numbers is set to be 1 in order to obtain high reduction ratio. As the tooth numbers of the gears are 121 and 120, respectively, 120 nutations cause a rotation. As the motor has three pneumatic cylinders, a nutation is achieved with six stepping motions for the half-pitch drive and with three stepping motions for full-pitch drive. Thus, the positioning resolution of the motor is 720 steps/rotation for the half-pitch drive and 360 steps/rotation for the full-pitch drive. Three solenoid on/off valves are used to generate pneumatic pulses. The motor specification is shown in Table 2.

4.2 Experiments

The developed motors were tested using a torque gauge and a powder brake for variable load. Three-bit pulse signals are generated by a personal computer and they drive the solenoid valves.

Figure 7 shows static characteristics of the motor driven by the full-pitch pressurizing pattern. Six prototypes were tested and the average data is shown. The experiments were conducted while keeping the rotational speed 2 rpm and increasing the load torque

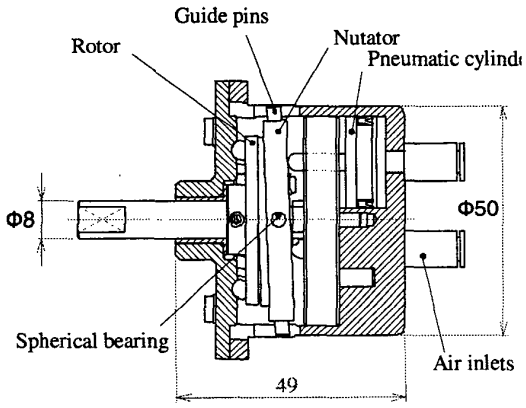

Fig. 4 Cross section of the motor

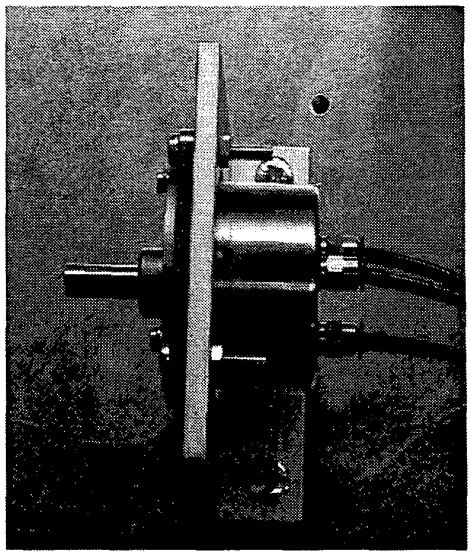

Fig. 5 Developed nutation motor

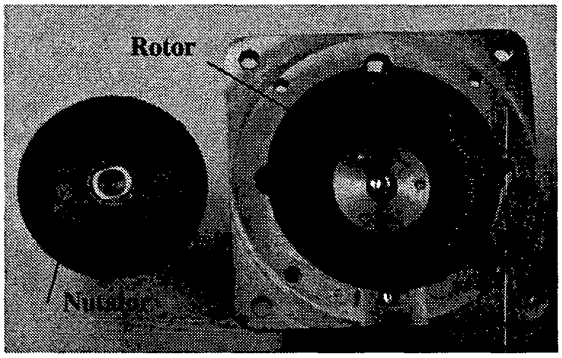

Fig.6 Nutator and rotor

from no load to find the critical torque at which ratcheting occurs. No slip was recognized and complete stepping motion was achieved with the load smaller than the critical torque. Ratcheting torque is almost proportional to the applied pneumatic pressure. The results calculated by Eq. (3)-(14) agree well with the experimental results.

Figure 8 shows the torque versus rotation for different length of the pneumatic tubes between the valves and the motors. Pneumatic pressure of 0.5 Mpa was applied.

Table 1 Specification of bevel gears

	rotor	nutator
Module	0.3 mm	
Pressure angle	20 deg.	
Tooth number	120	121
Tooth width	5 mm	
Axis angle	178 deg.	
Pitch circle	36	36.3
Tooth depth	0.675 mm	
Addendum	0.3 mm	
Dedendum	0.375 mm	
Cone distance	18.582 mm	
Pitch cone angle	75.628deg	102.372
Root tooth cone angle	74.472deg	101.216
Tip tooth cone angle	76.553deg	103.297

Table 2 Motor specification

Size [mm]	50 in diameter 49 in length
Weight [g]	650
Numbers of teeth	121 for nutator 120 for rotor
Torque [Nm]	2 max (experimental data)
Speed [rpm]	10 max (experimental data)
Step angle [deg]	0.5

The resolution of the rotor was found to be 360 steps/rotation for the full-pitch drive and 720 steps/rotation for the half-pitch drive.

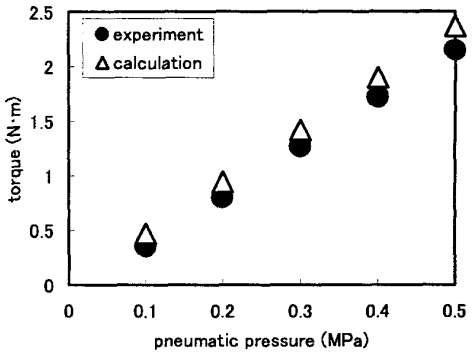

Fig. 7 Static characteristics of the motor
(full-pitch drive)

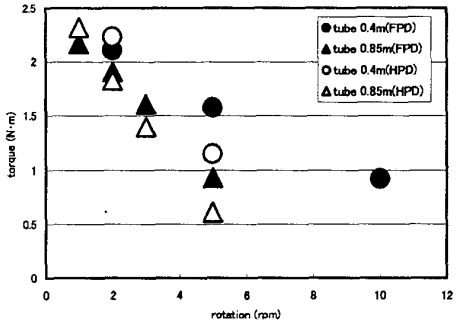

Fig. 8 Speed-torque characteristics of the motor
(pneumatic pressure 0.5 MPa)

5. Applying to parallel robot mechanism

The developed motors were applied to a robot mechanism to show the potential of the motor as a robot servo motor experimentally.

The robot is shown in Fig. 9. The design is based on HEXA robot [4], a parallel link robot with six degrees of freedom. Six pneumatic nutation motors were used. The six upper arms connect the lower arms and a table with universal joints. Dimensions of the robot are shown in Table 3.

Using a PC as a controller, the robot works successfully to control the table position x, y, z and

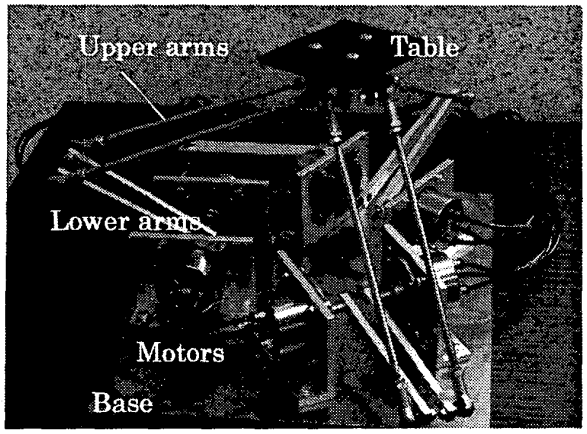

Fig. 9 Applying pneumatic nutation motors to parallel robot

orientations around *x*-, *y*-, *z*- axes. The robot specification is shown in Table 4.

Positioning accuracy of 1 mm to 2 mm was achieved without any electrical devices or sensors mounted on the robot.

6. Conclusions

A new type of pneumatic stepping motor, named pneumatic nutation motor was developed and its potential as a servo motor was shown by applying it to a parallel linkage robot with six degrees of freedom. This motor achieves stepping positioning of 720 steps/rotation without any electrical devices or sensors mounted on the servomechanisms.

While the positioning accuracy is not good with current design, the motor can be used under hazard conditions such as in water and in the strong magnetic fields where conventional electromagnetic motors cannot be used.

Table 3 Dimensions of the parallel robot

	Dimensions
Lower arms	142×12×6 mm
Upper arms	*l* 166mm、 ϕ 6.0mm
Moving table	90×90×6mm
Base table	300×350×6mm
Distance between arms	13mm

Table 4 Parallel robot specification

Working area	240 mm in *z*-axis, 210 mm in *x*-, *y*-axis
Load capacity	30 N
Positioning accuracy	1 mm in *x*-axis, *y*-axis 2 mm in *z*-axis

References

[1] K.Suzumori, K.Hori, and T. Miyagawa, A Direct-Drive Pneumatic Stepping Motor for Robots: Designs for Pipe-Inspection Microrobots and for Human-Care Robots, *Proc. IEEE International. Conf. on Robotics and Automation*, (1998), pp.3047-3052.

[2] H.Kimura, S.Hirose, and K. Nakaya, Development of the Crown Motor, Proc. ICRA, Seoul, pp.2442-2447 (2001).

[3] M. Uchiyama, A 6 d.o.f. parallel robot HEXA, ADVANCED ROBOTICS, The International Journal of the Robotics Society of Japan, 8-6 (1994), 601-601.